JOURNAL OF THEORETICAL AND APPLIED MECHANICS
51, 3, pp. 751-761, Warsaw 2013

ROBUST CONTROL OF THE MICRO UAV DYNAMICS WITH AN AUTOPILOT

Arkadiusz Mystkowski
Białystok University of Technology, Bialystok, Poland
e-mail: a.mystkowski@pb.edu.pl

This paper presents a nonlinear robust control design procedure for a micro air vehicle, which uses the singular value (μ) and μ-synthesis technique. The optimal robust control law that combines parametric and lumped uncertainties of the micro UAV (unmanned aerial vehicle) which are realized by serial connection of the Kestrel autopilot and the Gumstix microprocessor. Thus, the robust control feedback loops, which handle the uncertainty of aerodynamics derivatives, are used to ensure the robust stability of the UAV local dynamics in longitudinal and lateral control directions.

Key words: robust optimal control, *mu*-synthesis, uncertainty design, micro aerial vehicle, autopilot

1. Introduction

The control of dynamics of small air vehicles requires overcoming many characteristic features that are specific to these flying aircraft such as open-loop instability, very fast dynamics, nonlinear behaviour and high degree of coupling among different state vector elements. The dynamics of a micro aircraft has an uncertainty effect that causes variability of the model dynamics during the flight phases. The most sensitive are aerodynamics derivatives which change the micro air vehicle model. Most initial attempts to achieve stable autonomous flight have been based on PID controller design. Many commercial autopilots such as Procerus's Kestrel [11] or Micropilot's MP2128 [6] are based on PID controllers. The main advantage of PID control is that controller parameters may be easily adjusted when the model is not exactly known. This is a cheap and fast technique, where the PID controller parameters can be tuned on-line during the test flight. However, in spite of such advantages, the PID control method does not perfectly follow the system dynamics because of uncertainty in the aircraft dynamical forces and moments. Furthermore, the PID controllers are of the SISO type. It is assumed that controlled states are not strongly coupled.

In the paper, the robust optimal nonlinear control law that combines parametric and lumped uncertainties of the micro UAV (unmanned aerial vehicle) is investigated. The robust control feedback loops are used to ensure the robust stability of the UAV local dynamics in longitudinal and lateral control directions. The μ-synthesis robust control algorithms are calculated by using the robust control toolbox Matlab and optimized via fixed-point arithmetics [5]. The μ-synthesis controllers are of a high order, thus the real realization of the control code needs a powerful microprocessor. The considered micro air vehicle is supported with commercial, small Kestrel autopilot [11]. The Kestrel system includes software and control libraries. Meanwhile, this autopilot is not able to properly run such a high order control algorithms. Therefore, the optimized control algorithms in C++ language were implemented in the Gumstix Verdex Pro single-board microcomputer [14]. Then, the Gumstix was integrated with the autopilot to take control of the micro aerial vehicle (MAV) local dynamics. The micro aerial vehicle (MAV) based on single-delta wing configuration (BULLIT) with the Kestrel autopilot connected with the

external microcomputer was used as a control system. By using serial connection of the Kestrel autopilot supported by software codes and Gumstix microprocessor, the local control loops of the Kestrel are switched off and the external processor takes control of the micro plane. The way-point global control loop and Kalman filters of flight signals are realized by the Kestrel autopilot and are not investigated here. The hardware in the loop simulations results were presented due to tested robust control algorithms with using the real micro air vehicle with the Kestrel autopilot and Gumstix microprocessor. The developed controllers were proved to be efficient.

The hardware-in-the-loop simulations results were presented due to tested robust control algorithms with using the real micro aerial vehicle. The developed controllers proved to be efficient.

2. The BULLIT

The micro air vehicle (MAV) examined in this paper as the control plant is called BULLIT [15]. The single-delta wing MAV is equipped with the Kestrel autopilot and Gumstix Verdex Pro microprocessor electronics. The main MAV data are: wingspan of 0.84 m, weight "ready to flight status" 1.3 kg and the chord length of the NACA 0012 modification profile of 0.57 m. The control is accomplished using a set of aileron and elevator control surfaces. Thus, the airplane control system allows one to control the lateral-directional and longitudinal-directional dynamics. The full model has three control inputs: aileron, elevator and throttle. The aileron and elevator controls are realized by the Gumstix microprocessor, and the throttle control is evaluated by the Kestrel autopilot. The geometry data, model of motion and aerodynamics derivatives are provided by Mystkowski (2012a,b).

The measured outputs are the MAV states due to the body frame coordinates (X, Y, Z) (Fig. 1), and in the case of the lateral-directional control are: roll, roll rate, yaw rate and lateral velocity. Therefore, the state vector consists of (u, w, q, θ, h), where: u – velocity along X [m/s], w – velocity along Z [m/s], q – pitch rate [rad/s], θ – pitch angle [rad], and h – altitude [m]. The lateral state vector is given by (v, p, r, ϕ), where: v – velocity along Y [m/s], p – roll rate [rad/s], r – yaw rate [rad/s], and ϕ – roll angle [rad].

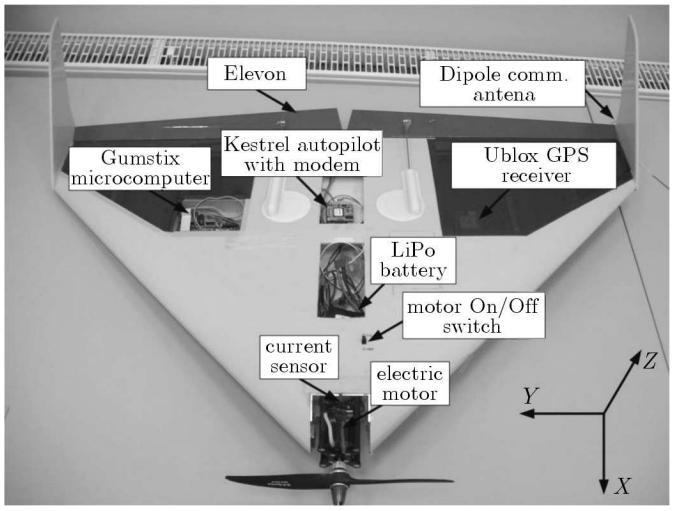

Fig. 1. BULLIT with Kestrel autopilot and Gumstix microprocessor – during assembling

3. Sensitivities of micro UAV

The aerodynamics of the micro unmanned aerial vehicles are usually determined using a low speed free-stream velocity of 10-20 m/s and the Reynolds number of 10 000-100 000. The Reynolds

number, small size of geometry and low weight causes the vehicle model extremely difficult to identify. The micro wings-level study to consider, e.g. sweeps across the angle of attack and/or angle of sideslip are often poor in facility. The computation of static derivatives in the pitch, roll and yaw does not allow one to predict the derivatives variations. Moreover, the variations of the UAV forces and moments with respect to the time rates of change of the angle of attack and angle of sideslip can not be estimated. Consequently, the UAV measured data obtained in the wind tunnel is not sufficient to completely characterize the UAV flight dynamical model. Thus, the facility did not allow one to estimate the dynamical derivatives.

In the paper, the wind tunnel data and numerical calculations performed for BULLIT denoted some anomalies in aerodynamics. The experimental measurements were performed in an open-wind tunnel (Mystkowski and Ostapkowicz, 2011). The aerodynamics numerical computations were performed in the Tornado-Matlab and the XFLR5 software by using the Vortex Lattice Method (Gordnier, 2009; [10], [12]). These analyses assume incompressible and not viscid flow, which generate some errors in the resulting solution. A set of static and dynamic lateral/longitudinal derivatives are calculated at a given flight condition presented in Table 4. In particular, the lift/drag coefficients due to angle of attack derived in wind tunnel do not agree with the simulation results (see Figs. 2a,b).

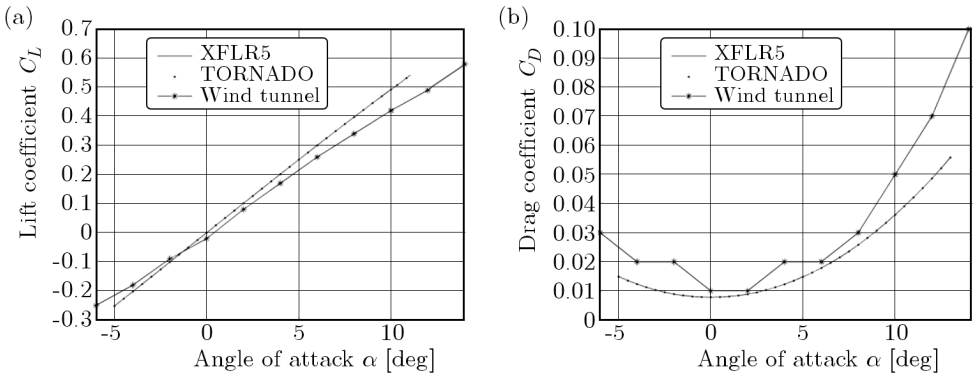

Fig. 2. (a) Lift coefficient, (b) drag coefficient

The micro UAVs are characterized by their instability and nonlinearity, e.g. turbulence flow, air vortex along lifting surfaces, low stall speed, high sensitivity to external flight disturbances and more. Also, the variations of the UAV forces and moments with respect to flight conditions are difficult to predict. Therefore, to include these properties, some tools of the robust optimal method with a structural singular value are used (Zhou *et al.*, 1996; Zhou and Doyle, 1998).

The structure of the micro UAV model (including the order) is usually known, but some of the parameters may be uncertain (Aguiar and Hespanha, 2007). The UAV model is in error because of missing dynamics. It is caused by unmodeled or neglected dynamics, usually at high frequencies. The UAV model is nonlinear, thus, the poor model accuracy is caused by unmodeled physical air-flow processes. The description of these parameters/model perturbations is presented here and denoted as a parametric and lumped uncertainty. The uncertainty analysis allows one to determine the UAV uncertainty model. Then, the uncertainty model of the UAV local dynamics is handled by using the μ-synthesis control (Balas *et al.*, 1991; Zhou *et al.*, 1996).

3.1. Parametric uncertainty

In this section, the stability test of the nominally stable UAV local dynamics under parameter variations, is considered. The UAV dynamical parameters, which are not stationary, are formulated and called here as parametric uncertainties. The parametric uncertainty means that the structure of the UAV model is known, but some parameters are uncertain. The uncertainties

of the UAV selected parameters are introduced/joined into the UAV model during the design of the μ-synthesis controller. The basis for the robust stability criteria for the UAV uncertain system is the so-called *small gain theorem* (Zhou and Doyle, 1998).

Based on the small gain theorem, for the internal family $P(s)$ of strictly proper control plants (where $C(s)$ is the stabilizing controller) the closed-loop system can be stable for all perturbations of control plant (denoted here as $\Delta P(s)$) such that

$$\|\Delta P(s)\|_\infty < \gamma \iff \sup \left\| [1 + P(s)C(s)]^{-1} C(s) \right\|_\infty < \gamma^{-1} \tag{3.1}$$

where γ is a positive constant coefficient that is equivalent to the largest singular value of the uncertainty matrix (introduced in 3.2).

Equation (3.1) can be rewritten in the form

$$\forall \Delta \in \mathbb{R}H_\infty \quad \text{where} \quad \|W_\Delta^{-1}\Delta\|_\infty < 1 \quad \text{if} \quad \|W_\Delta f(P,C)\|_\infty \leqslant 1 \tag{3.2}$$

where Δ is the uncertainty (bounded perturbation), H_∞ – frequency H-infinity norm, W_Δ – boundary function (uncertainty shaping function), $f(P,C)$ – closed-loop function, C – robust stabilizing controller and P – augmented control plant (including a nominal model and uncertainties).

Suppose $M(s) = W_\Delta f(P,C)$ and $M \in \mathbb{R}H_\infty$, then the UAV dynamics system is well posed and internally stable for all $\Delta(s) \in \mathbb{R}$ or $\Delta(s) \in \mathbb{R}H_\infty$ or $\Delta(s) \in \mathbb{C}^{qxp}$ with

$$\|\Delta\|_\infty \leqslant \gamma^{-1} \iff \|M(s)\|_\infty < \gamma \tag{3.3}$$

Meanwhile, for a good representation of the actual UAV local roll/pitch-axes dynamics by the nominal model P_0, the uncertainty model Δ should be as small as possible. The UAV "real/true" parameters K_i consist of the nominal values K_{i0} and their parametric uncertainties δ_i and are given in the following form

$$K_i = K_{i0} + W_{\Delta i}\delta_i \quad \text{for} \quad |\delta_i| \leqslant 1 \tag{3.4}$$

In this paper, only the UAV derivatives (parametric) uncertainties are investigated. Meanwhile, the prediction of these variability is highly challenging. The prediction uncertainty ranges (the UAV derivatives accuracy) for the longitudinal and lateral selected derivatives are shown in Table 1.

3.2. Lumped uncertainty

The lumped uncertainty represents one or more sources of the unmodelled dynamics and/or parametric uncertainty combined into a single lumped perturbation given in Fig. 3. Figure 3 presents the single channel μ-synthesis control loop for the UAV local dynamics. The weighting functions $W_e, \ldots, W_y$ are explained in Mystkowski (2012a,b).

The uncertainty here was introduced to the nominal UAV model in the multiplicative way. The structured multiplicative uncertainty ΔM for the nominal control model P_0 and the "true" augmented model P is given by Zhou and Doyle (1998)

$$|\Delta_M(j\omega)| = \frac{|P(j\omega) - P_0(j\omega)|}{P_0(j\omega)} \tag{3.5}$$

where

$$|\Delta_M(j\omega)| \leqslant 1 \quad \forall\omega \;\Rightarrow\; \|\Delta_M\|_\infty \leqslant 1 \tag{3.6}$$

Table 1. BULLIT derivatives – nominal values and their uncertainties

Longitudinal derivatives	Nominal value	Uncertainty [±%]	Lateral derivatives	Nominal value	Uncertainty [±%]
CL_α	2.61100	5	CY_β	−0.20707	10
CD_α	0.14762	5	Cl_β	0.04342	10
Cm_α	−0.71274	5	Cn_β	−0.05729	10
CL_u	0.10230	30	CY_P	0.10814	20
CD_u	0.02860	30	Cl_P	−0.14521	20
Cm_u	0.03270	30	Cn_P	0.02744	20
CL_Q	4.34620	30	CY_R	−0.13474	10
CD_Q	0.22854	30	Cl_R	0.02744	10
Cm_Q	−1.83640	30	Cn_R	−0.03765	10
Longitudinal control derivatives	Nominal value	Uncertainty [±%]	Lateral control derivatives	Nominal value	Uncertainty [±%]
$CL_{\delta e}$	1.11110	5	$CY_{\delta a}$	−0.05213	1
$CD_{\delta e}$	0.05939	0	$Cl_{\delta a}$	0.12987	5
$Cm_{\delta e}$	−0.68376	5	$Cn_{\delta a}$	−0.01192	5

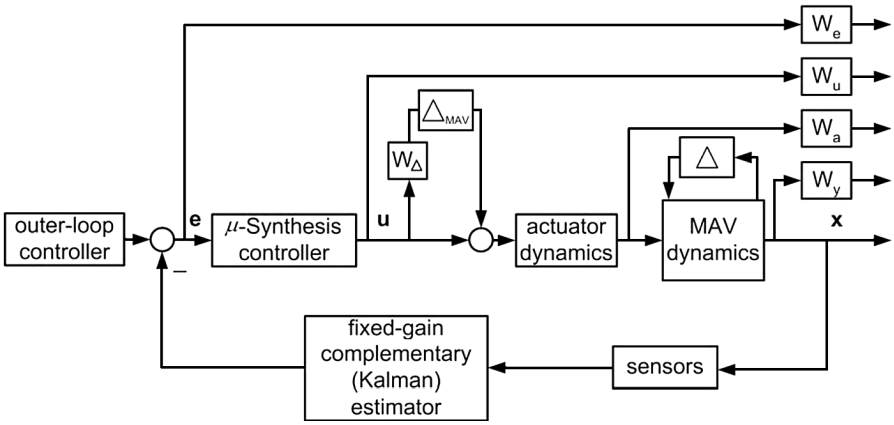

Fig. 3. Single channel μ-synthesis control loop

The structural singular value (denoted SSV or μ) is a function which provides a generalization of the singular value and its upper bound $\overline{\sigma}$. The μ is used to determine the robust stability and robust performance of the UAV dynamics. The definition of μ is given by (Zhou and Doyle, 1998)

$$\mu(M) := \frac{1}{\min\{\overline{\sigma}(\Delta):\ \Delta \in \mathbf{\Delta},\ \det(I - M\Delta)} = 0 \tag{3.7}$$

Then, the uncertainty is limited by bound

$$\overline{\sigma}\left(M(j\omega)\right) < \mu \tag{3.8}$$

The UAV dynamics model uncertainty data are collected in Table 2.

The some plots resulting from the combination of Δ and the uncertainty shaping function are presented in Fig. 4.

Table 2. Model uncertainty for pitch/roll control and pitch weights data

Name	Type
Uncertainty type	Structured/multiplicative
Error dynamics gain across frequency (bound)	< 1
Sample state dimension of error dynamics	5
UAV model uncertainty influence	10% up to 10 Hz and 100% over 10 Hz
Uncertainty shaping function model: gain – $M_\Delta = 10$, cut-off frequency – $\omega_\Delta = 10 \cdot 2pi$, bound – $e_\Delta = 0.5$	$W_\Delta(s) = \dfrac{s + \omega_\Delta M_\Delta^{-1}}{e_\Delta s + \omega_\Delta}$
Pitch uncertainty weight	$W_\Delta(s) = \dfrac{s + 6.283}{0.5s + 62.83}$
Pitch error signal weight	$W_e(s) = \dfrac{0.2941s + 62.83}{s + 0.6283}$
Pitch control signal weight	$W_u(s) = 1$
Measured signal weight	$W_y(s) = \dfrac{6672}{s^2 + 98.02s + 6672}$
Pitch actuator weight	$W_a(s) = \dfrac{0.3491s}{s + 0.3491}$

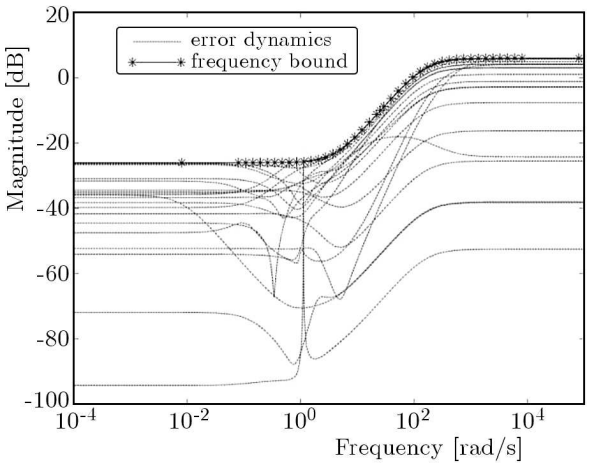

Fig. 4. Bode plot of UAV perturbations and uncertainty weight

4. Robust control system data

In order to design the μ-synthesis controllers for the UAV dynamics, the robust stability performances should be determined by using the weighting functions. The selected robust performances of the UAV control model are presented in Table 3.

The UAV nominal model data is denoted here as the nominal state, and is given in Table 4.

5. The μ-synthesis decoupled control model

The dynamics of the UAV/MAV was decoupled due to the control axis, and the lateral/longitudinal single channel flight controllers are designed (see scheme, Fig. 6). Therefore, the μ-synthesis controllers are simplified to SISO models. The lateral and longitudinal dynamics of the aileron and elevator vectors of the MAV are considered due to the state vector described in Section 2.

Table 3. Robust performances of the UAV μ-synthesis control system

Parameter	Nominal value	Upper/lower limits
Error signal pitch/roll	–	± 0.34 rad
Command signal pitch/roll	–	± 0.30 rad
Estimated roll/pitch	–	± 3.14 rad
W_e function slope	-2	
W_u and W_y function slope	$+2$	
Cut-off frequency for command signal (Gumstix serial port)	10 Hz	
Cut-off frequency for command signal (Kestrel local loops)	50 Hz	
Aileron/elevator deflection rate	–	0.69 rad/s
Aileron/elevator deflection	–	± 0.34 rad

Table 4. BULLIT, the nominal state

Parameter	Nominal value	Parameter	Nominal value
UAV total mass	1.270 kg	Wingspan	0.840 m
Air speed	15 m/s	Wing chord	0.570 m
Altitude	100 m	Outer chord	0.135 m
Trim angle of attack	0.087 rad	Area of the wing	0.296 m^2
Trim sideslip angle	0 rad	Area of the propeller	0.033 m^2
Trim pitch angle	0 rad	Taper ratio	0.236
Inertia moments: $I_{xx}/I_{yy}/I_{zz}/I_{zx}/I_{xy}/I_{yz}$	0.0184/0.0367/0.0550 $/-0.00021/0/0$ kgm^2	MAC	0.397 m

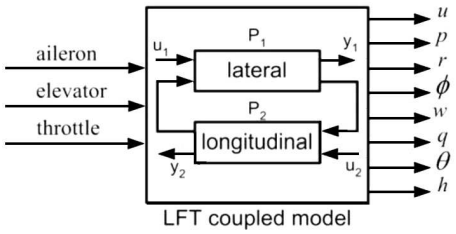

Fig. 5. Decoupled MAV I/O control model

The μ-synthesis control method enables the design of a multivariable optimal robust controller for complex linear systems with any type of uncertainties in their structure (Balas *et al.*, 1991; Valavanis, 2007; Zhou *et al.*, 1996; Zhou and Doyle, 1998). The μ-synthesis controllers were calculated by using the tools of Robust Control Toolbox$^{\mathrm{TM}}$ of Matlab [5]. The command *dksyn* allows one to perform the synthesis and set the frequency grid used for the μ-synthesis. The μ-controller is calculated during the recurrence algorithm, which seeks a matrix $\mathbf{D}$, until the following condition is met (Zhou and Doyle, 1998)

$$\|\mathbf{D}T_{y_1u_1}\mathbf{D}^{-1}\|_\infty \leqslant 1 \tag{5.1}$$

where: $\mathbf{D} = \mathrm{diag}\Big(d_1(s)I_{k_1}, \ldots, d_n(s)I_{k_n}\Big)$, and $T_{y_1u_1}$ – closed loop function.

The μ-controller optimizes the following cost function (Zhou and Doyle, 1998)

$$\mu = \min_{D(j\omega)} \overline{\sigma}\Big(\mathbf{D}(j\omega)T_{y_1u_1}(j\omega)\mathbf{D}^{-1}(j\omega)\Big) \tag{5.2}$$

The μ-controller synthesized for the augmented plant model P must meet the analysis objectives presented by the maximal singular value μ (see Section 3.2). The control structure of

the UAV with the Kestrel autopilot, serial communication, external processor, and the robust controller, is presented in Fig. 6.

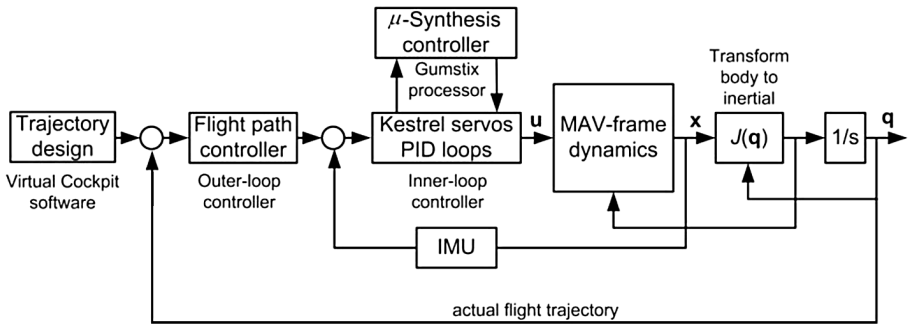

Fig. 6. Basic cascade μ-synthesis control structure

6. The μ-synthesis algorithm implementation in Gumstix microcomputer

The μ-synthesis controllers for lateral and longitudinal (pitch/roll only) control feedback-loops are of the 6th order. In order to implement the robust optimal controller in the Gumstix microprocessor, the control algorithm should be realized using the digital representation with the fixed sample period T. The discrete time models of the μ-synthesis and their coefficients b_n/a_m were found using a difference equation method (Burns, 2001). In this method, all of the subsequent differentials of the control signal $u(t)$ and the error signal $e(t)$ were discretized for the i-th time step by using a well known formulae

$$\frac{du}{dt} \approx \frac{u(i) - u(i-1)}{T} \tag{6.1}$$

The frequency of packet data flow between the Kestrel autopilot and Gumstix was 10 Hz. Therefore, the robust control algorithms were discretized with the sample time which equals 0.1 s. These algorithms are written in form of the Z transform as

$$\frac{u_0}{e_i}(z) = \frac{b_0 + b_1 z^{-1} + \ldots + b_6 z^{-6}}{1 + a_0 + a_1 z^{-1} + \ldots + a_6 z^{-6}} \tag{6.2}$$

Equation (6.2) can be presented as a microprocessor implementation (for the k-th time step) in the form

$$u_0(kT) = -a_1 u_0(k-1)T - \ldots - a_6 u_0(k-6)T + b_0 e_i(kT) + b_1 e_i(k-1)T + \ldots + b_6 e_i(k-6)T \tag{6.3}$$

The structures of aileron and elevator control loops for the UAV (by using a serial connection between the Kestrel autopilot and Gumstix processor) are presented in Figs. 7 and 8.

7. Hardware in the loop results

The hardware in the loop simulation uses a real aircraft with an autopilot where the flight environment is simulated [11]. This software and hardware connection enables one to verify the control strategy. The hardware communication block diagram for normal flight (wireless) and during the simulation state (serial cable connection) are given in Figs. 9 and 10.

The HIL simulation uses the Aviones software to simulate the flight conditions and environment [11]. In order to increase the model accuracy simulated in the Aviones, some modification have been made to the Aviones configuration files. The results of the roll/pitch up manoeuver are

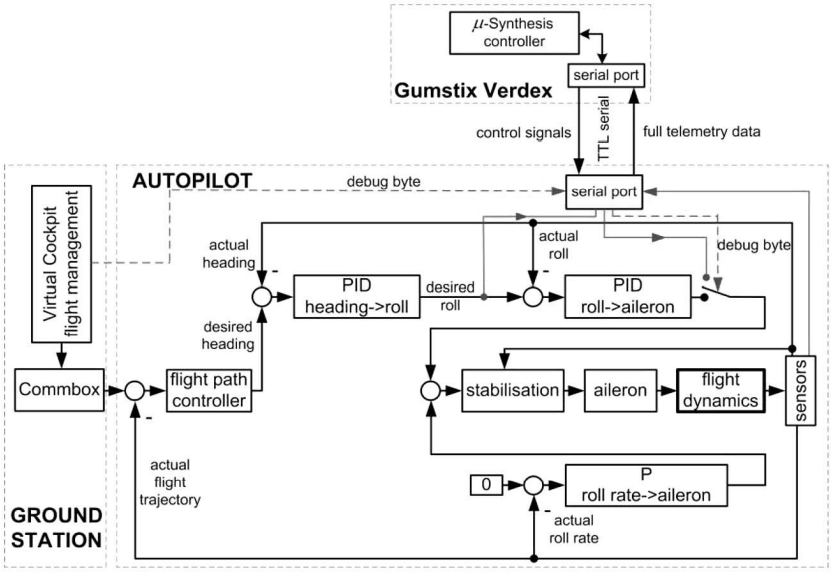

Fig. 7. Gumstix-Kestrel aileron μ-synthesis control feedback loop

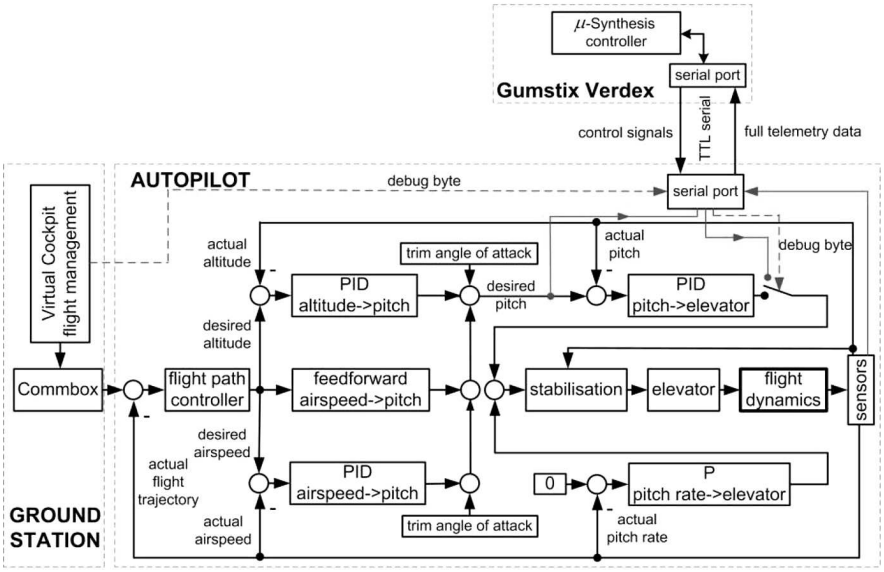

Fig. 8. Gumstix-Kestrel elevator μ-synthesis control feedback loop

shown in Figs. 11 and 12. The state was recorded by the logger of the flight/telemetry data with the frequency of 5 Hz. Figure 11 shows that the *mu*-controller has met the robust performances specs due to the UAV derivatives uncertainties. The measured roll angle follows the desired value, where the aileron stick control energy is minimalized. The overshot and control errors are limited due to simulated wind disturbances. The μ-synthesis control properties were compared with the PID control. The PID control algorithm was tested as originally implemented by the Lockheed Martin Procerus in Kestrel autopilot. As can be seen, the aileron stick signal during PID control has a bigger amplitude than the aileron stick signal generated by the μ-synthesis controller. For the μ-synthesis control the aileron deflection angle limit was set by the weighting functions. The two states (see Figs. 11 and 12), when the roll angle equals to $29°$, were recorded during the UAV aileron commands. However, in Fig. 11, there is some delay introduced by the serial connection of Gumstix and Kestrel autopilot. This delay is forced by the low frequency of the data packet exchange which is limited to 10 Hz.

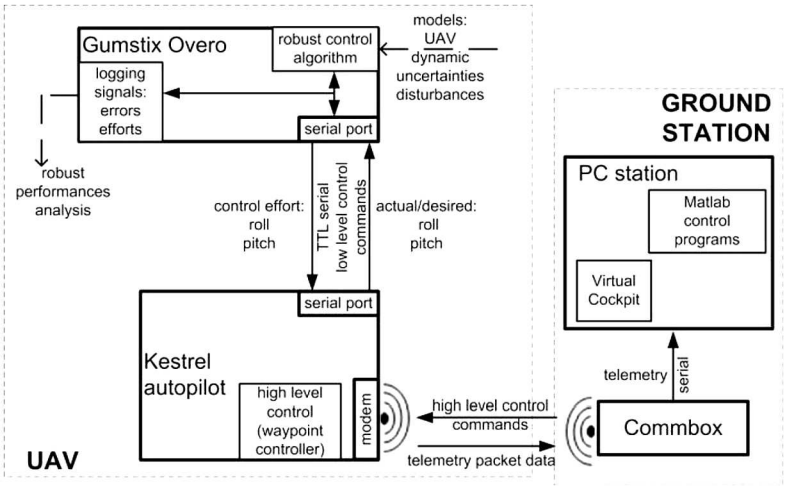

Fig. 9. Communication during normal flight

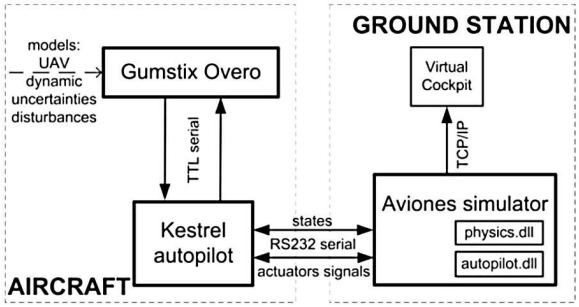

Fig. 10. Communication during HIL

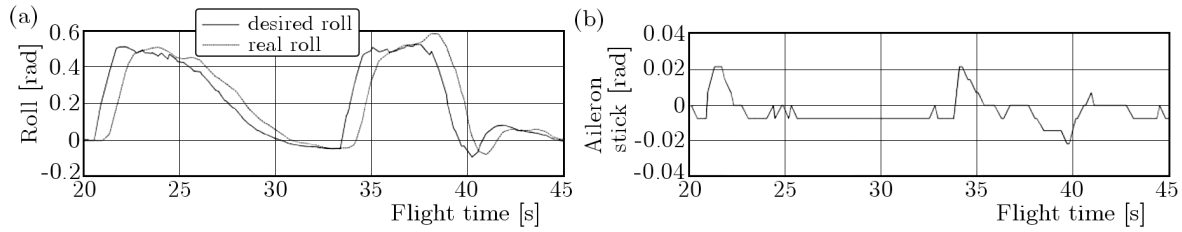

Fig. 11. HIL, μ-synthesis roll control

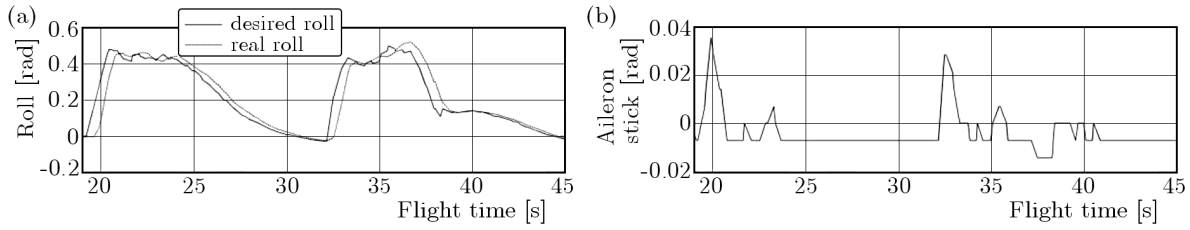

Fig. 12. HIL, PID roll control

8. Summary and conclusion

The very short specifications of the BULLIT UAV are introduced in the first Section. Next, the UAV parameters variations are presented as the uncertainty models. The lumped UAV uncertainty was investigated and introduced to the control loop in a multiplicative way. The robust control system structure with weighting functions, which are used to meet the robust

performances, is presented. Then, the robust control system data for the micro UAV are given. Next, the μ-synthesis decoupled control design and digital implementation are performed for the uncertain model of the UAV. Finally, the control feedback loop structure and results of the hardware in the loop tests are shown and commented.

The longitudinal/lateral-directional control loops of the UAV use the decoupled μ-synthesis control law. The μ-synthesis controllers were performed to check if the specs can be met robustly when taking into account the uncertainty Δ. These controllers can keep the closed-loop gain below $\mu = 0.89$ for the specified parameters uncertainty. This indicatives that the robustness specs can be fully met for the family of the aircraft models. The design goal was to develop the "true" UAV model, for which the response to the longitudinal stick agrees well with the real response.

References

1. Aguiar A.P., Hespanha J.P., 2007, Trajectory-tracking and path-following of underactuated autonomous vehicles with parametric modeling uncertainty, *IEEE Tran. on Automation Conference*, **52**, 1362-1379
2. Balas G.J., Packard A.K., and J.T. Harduvel J.T., 1991, Application of μ-synthesis techniques to momentum management and attitude control of the space station, *AIAA Guidance, Navigation and Control Conference*, New Orleans
3. Burns R.S., 2001, *Advanced Control Engineering*, Butterworth-Heinemann
4. Gordnier R.E., 2009, High fidelity computational simulation of a membrane wing airfoil, *Journal of Fluids and Structures*, **25**, 897-917
5. Mathworks Inc., www.mathworks.com
6. Micropilot Inc., www.micro-pilot.com
7. Mystkowski A., 2012a, An application of μ-synthesis to control of a small air vehicle – simulation results, *Journal of Vibroengineering*, **14**, 1, 79-86
8. Mystkowski A., 2012b, The robust control of unmanned aerial vehicle, *Research project report No, 0029/R/T00/2010/11*, conducted in the years: 2010-2013 [in Polish]
9. Mystkowski A., Ostapkowicz P., 2011, Verification of MAV dynamics model with vortex piezo-generators to boundary flow control, *Warsaw Inst. of Aviation*, **216**, 103-125
10. NASA, 1976, *Vortex-lattice utilization*, NASA SP-405, NASA-Langley, Washington
11. Procerus, Inc., www.procerus.com
12. Tornado 1.0, 2001, *User Guide, Reference manual*, Relase 2.3
13. Valavanis K.P., 2007, *Advances in Unmanned Aerial Vehicles, State of the Art and the Road to Autonomy*, Springer, 33
14. www.gumstix.com
15. www.topmodelcz.cz
16. Zhou K., Doyle J., 1998, *Essentials of Robust Control*, Prentice Hall
17. Zhou K., Doyle J.C., Glover K., 1996, *Robust and Optimal Control*, Prentice Hall

Manuscript received May 29, 2012; accepted for print January 14, 2013